BUCKLING OF FIBER REINFORCED COMPOSITE PLATES WITH NANOFIBER REINFORCED MATRICES

Christos C. Chamis, Ph.D. and Pappu L.N. Murthy, Ph.D.
NASA Glenn Research Center
Cleveland, OH 44135, USA
Christos.C.Chamis@nasa.gov

ABSTRACT

Anisotropic composite plates were evaluated with nanofiber reinforced matrices (NFRM). The nanofiber reinforcement volumes ratio in the matrix was 0.01. The plate dimensions were 20 by 10 by 1.0 in. (508 by 254 by 25.4 mm). Seven different loading condition cases were evaluated: three for uniaxial loading, three for pairs of combined loading, and one with three combined loadings. The anisotropy arose from the unidirectional plates having been at 30° from the structural axis. The anisotropy had a full 6 by 6 rigidities matrix which were satisfied and solved by a Galerkin buckling algorithm. The buckling results showed that the NFRM plates buckled at about twice those with conventional matrix.

1. INTRODUCTION

Considerable research activities in nanocomposites have been actively pursued recently. One aspect of this research is on nanofiber reinforced matrices (NFRM) which can subsequently be used as matrices in conventional reinforced fiber composites. As of to date, the buckling of composite plates with NFRM has not been investigated yet. This is the objective of the present paper, to use a commercial composites loaded at 30°(Fig.1) from the material axis for seven different cases. The results are compared with fiber composite without the NFRM that is an AS/IMHS (AS graphite fiber/intermediate modulus high strength matrix) for all the loading conditions. Because the 30° off-axis composite has a full 6×6 bending stiffness matrix, a Galerkin algorithm is used to evaluate the buckling factor. The bending stiffness required for the buckling of off-axis loaded anisotropic composite were generated by the in-house integrated computer code in composite mechanics. The comparison of results without and with the NFRM show about twice the buckling factor for all loading conditions with only 1 percent of nanofiber reinforced matrix. Results are presented for the buckling factor mode and its corresponding buckling factor for each loading condition. The graphical results shown will be for the type of loading condition, the 3–D buckling factor mode shape, a contour plot of the buckling factor mode and a convergence plot of the buckling algorithm. One interesting result is that the shear buckling factor does not converge and requires a tiny small loading in one or both structural axes to enhance the convergence.

The theory was developed when the first author was a graduate student at Case Western Reserve University and it is described in Reference 1. The application to the anisotropic plates was performed when he started working at NASA Lewis Research Center (now Glenn Research Center) Reference 2. The programming details source code and several sample cases are in the appendices of Reference 2. The brief description of the theoretical background is from Reference 2 also.

The underlying theory for buckling factors of anisotropic plates is described in References 1 and 2 with pertinent discussions in References 3 to 5. Briefly, this theory consists of expressing the potential energy of plate in terms of displacement variables. Taking the variation of the potential energy function yields the field equation and the corresponding boundary conditions. The resulting system then is solved by the assumed mode technique in conjunction with the Galerkin method (Fig. 2).

The equation resulting after the variation of the energy function is

$$\begin{aligned}\int_0^a\int_0^b \Big[& D_{11}w_{,xxxx} + 2(D_{12}+2D_{33})\,w_{,xxyy} + D_{22}w_{,yyyy} + 4D_{13}w_{,xyxx} \\ & + 4D_{23}w_{,xyyy} - \left(\overline{N}_X w_{,xx} + 2\overline{N}_{xy} w_{,xy} + N_y w_{,yy}\right)\Big]\,\delta w\,dy\,dx \\ & + \int_0^b \Big(D_{11}w_{,xx} + D_{12}w_{,yy} + 2D_{13}w_{,xy}\Big|_0^a \delta w_{,x}\,dy \\ & + \int_0^a \Big(D_{21}w_{,xx} + D_{22}w_{,yy} + 2D_{23}w_{,xy}\Big|_0^b \delta w_{,y}\,dx = 0\end{aligned} \tag{1}$$

(The notation is defined in Appendix A of Reference 2.) The area integral represents the field equation, and the line integrals represent the boundary conditions.

The assumed buckling factor mode described in Reference 2 is represented by a Fourier double sine series. This mode satisfies the imposed boundary conditions, but it does not satisfy the natural boundary conditions if the material and structural axes do not coincide. However, the mode is forced to satisfy the natural boundary conditions approximately through the Galerkin method as discussed in Reference 2.

Substituting the assumed mode in Equation (1), applying the Galerkin method, and carrying out the algebra result in a set of linear equations

$$[K]\,\{w\} = \lambda\,[L]\,\{w\} \tag{2}$$

where K is the stiffness matrix, λ is the eigenvalue [L] is the loading matrix and {w} is the displacement vector which represent the eigenvalue problem of the plate. This system is coupled for either a combination of shear and normal loads and/or noncoincident material and structural axes.

The eigenvalue problem is solved by using the Power method, which is a highly effective iterative numerical technique in seeking the largest eigenvalue of the system. The indicial equations which were used to generate this system and the Power method are given in Appendix B of Reference 2 in outline form.

The source code has been reprogrammed by Dr. Murthy in Metlab. The buckling results presented subsequently are from the Metlab reprogrammed. There are two portions to the results: (1) is the simulation of the NFRM which is performed by a composite mechanics code ICAN/JAVA in order to obtain the nanofiber reinforcement in the matrix and (2) using the

NFRM in the mechanics computer code again to simulate the effects of the reinforced matrix in the buckling behavior of the composite plate for different combination of loads.

The nanofiber reinforced matrix (NFRM) is simulated by using the nanofiber properties shown in Table 1 in an intermediate modules high strength matrix in Table 2 assuming a quasi isotropic fiber arrangement. The properties of this lay-up arrangement are shown in Table 3. Next, the conventional fiber in Table 4 was used with the NFRM to obtain the bending rigidities shown in Table 5.

2. RESULTS AND DISCUSSION

The composite plate shown in Figure 1 was selected for the buckling evaluation. The fiber reinforcement was 0.6 volume ration in a NFRM. The bending rigidities shown in Table 5 were transformed to 30° from the structural x-axis to obtain the anisotropic composite plate. The transformed rigidities were input into the buckling routine with the plate geometry (20×10×1.0) length, width, thickness and the results were obtained for seven different cases of combined in plane loads. For convenience all the inplane loads were assumed to be of equal magnitude. Two different buckling results are shown for conventional matrix Table 6 and for NFRM Table 7.

The buckling factor conditions indicated in each table with a check mark. Note that the structural axis has only one check mark in the first column. The y axis has one check mark in the second column. The x-y loading has a check mark in the third column combined load cases leave check marks in the appropriate column to indicate the combined loading.

Comparing the buckling results of the two tables it is seen that the plates with the NFRM is about twice of the conventional matrix.

3. BUCKLING FACTOR MODE SHAPES

The buckling factor mode shapes of anisotropic plates is very interesting. In this evaluation buckling factor mode shapes were evaluated for each loading condition that means there are seven charts of buckling factor mode shapen. Each chart has four parts in it. The top left (a) is a contour part of the modal shape. The upper left (b) is a 3–D view of the buckling factor mode shape. The lower left (c) is a buckling factor convergence plot. The lower right (d) is a box with the following information in it: first line loading conditioning, second line, load axis; third line the buckling factor of that case.

Part (a) in Figure 3(a) depicts the contour plot of the buckling factor mode shape for buckling factor in the x direction. Part (b) depicts a 3–D presentation of the buckling factor mode shape. Part (c) depicts the buckling factor convergence in 8 interactions. Part (d) is the box with all the information of the mode shape. Note that the plate buckled in two modes. The buckling factor is 3673 lb (163.38 kN).

Figure 4 depicts analogous information or the buckling factor in the transverse direction. Part (a) is the contour plot; part (b) is the 3–D view of the mode shape; part (c) is the convergence plot in 6 interactions and part (d) is the buckling information box. The buckling factor is 1097 lb. (48.79 kN).

Figure 5 depicts similar information of the shear load buckling shape. Note that this mode shape symmetric about the material axis 30° from the x axis. Note that buckling factor converged in 7 interactions. Note also that the very small load of 1 lb (4.448 N) in the x- and y-axis as was previous explained. The buckling factor is 2220 lb. (98.75 kN).

Figure 6 depicts the buckling factor mode shape of bi-axial combined loads. Note that this contour plot depicts a symmetric mode shape about the material axes also. Note also the buckling factor converged in 6 iterations as well. The buckling factor is 875 lb. (3.892 kN).

Figure 7 is the buckling factor mode shape of combined buckling factor axial and shear. The contour plot of this mode shape also is symmetric about the material axis. Note the buckling factor converged in 7 iterations. The buckling factor is 1520 lb. (6.761 kN).

Figure 8 is the buckling factor mode shape of a y-axis and shear load. As was the case previously the contour plot show symmetry about the material axis. The buckling factor converged in 8 iterations with a value of 808 lb. (35.94 kN).

Figure 9 depicts the buckling factor mode shape of combined loads x, y, and xy. The buckling factor converged in 8 iterations to a value of 680 lb. (30.25 kN).

4. CONCLUDING REMARKS

The concluding remarks of a buckling of anisotropic composite plates with NFRM are as follows. The nanofiber reinforcement has a major effect in the buckling factor. All the cases investigated for combined loads showed the same about twice benefit compared to conventional matrix. All buckling factor mode shape were single except the one loaded alone the structure x-axis which had double mode. All buckling factor mode contour plot showed symmetry about the matrix axis except the first case which showed symmetry about 45° to the structural x-axis. The shear loading only case required a small load in the two other orthogonal axes to expedite convergence. All buckling factor converged between 6 and 8 iterations. The buckling algorithm is very effective and its convergence is efficient. The simulation of the nanofiber reinforced matrix is also an effective means to obtain the influence of nanofibers in a matrix first and then combine the NFRF with the conventional fibers for other structural evaluations.

5. REFERENCES

1. Chamis, C.C.: Buckling of Anisotropic Composite Plates. J. Structural Div., ASCE, vol. 95, no. ST10, Oct. 1969, pp. 2119–2139
2. Chamis, C.C.: Theoretical Buckling Loads of Boron/Aluminum and Graphite/Resis Fiber-Composite Anisotropic Plates. NASA TN D-6572, December 1971.
3. Wang, James T.-S.: On the Solution of Plates of Composite Materials. J. Composite Mat., vol. 3, July 1969, pp. 590–592.
4. Hsu, T.M.: Buckling of Anisotropic Plates, Discussion J. Structural Div., Am. Soc. Civil Eng., vol. 96, no. ST7, July 1970, p. 1604.
5. Chamis, C.C.: Buckling of Anisotropic Plates, Closure and Errata. J. Structural Div., Am. Soc. Civil Eng., vol. 97, no. ST3, Mar. 1971, p. 960.

TABLE 1.—NANOFIBER (TRIAL FIBER)
[TRIAL FIBER MODULUS 123M FOR SINGLE FIBER 3–D STRESS ANALYSIS.]

Description	Symbol	Value	Value in SI units
Number of fibers per end	Nf	100.0	100
Filament equivalent diameter	df	4.0×10^{-10} in.	1.016×10^{-8} mm.
Weight density	Rhof	0.06 lb/in.^{3}	1.661×10^{-6} kg/mm^3.
Normal moduli (11)	Ef11	1.0×10^{9} psi	689.5×10^{10} Pa
Normal moduli (22)	Ef22	41.0×10^{7} psi	282.7×10^{10} Pa
Poisson's ratio (12)	Nuf12	0.2 non-dim.	0.2 non-dim.
Poisson's ratio (23)	Nuf23	0.35 non-dim.	0.35 non-dim.
Shear moduli (12)	Gf12	2.0×10^{7} psi	13.79×10^{10} Pa
Shear moduli (23)	Gf23	1.5×10^{7} psi	10.34×10^{10} Pa
Thermal expansion coefficient (11)	Alfaf11	-6.0×10^{-8} in./in./°F	-10.8×10^{-8} /°C
Thermal expansion coefficient (22)	Alfaf22	6.0×10^{-6} in./in./°F	10.8×10^{-6} /°C
Heat conductivity (11)	Kf11	400.0 BTU/hr/in./°F	8.3075 W/mm/°C
Heat conductivity (12)	Kf12	40.0 BTU/hr/in./°F	0.83075 W/mm/°C
Heat capacity	Cf	0.17 BTU/lb/°F	712.3 J/kg/°C
Dielectric strength (11)	Kef11	0.0 V/in.	0.0 V/mm
Dielectric strength (22)	Kef22	0.0 V/in.	0.0 V/mm
Dielectric constant (11)	Gammaf11	0.0 in./V	0.0 mm./V
Dielectric constant (22)	Gammaf22	0.0 in./V	0.0 mm./V
Capacitance	Cef	0.0 V	0.0 V
Resistivity	Ref	0.0 Ω-in.	0.0 Ω-mm
Tensile strength	SfT	1000000.0 psi	6895×10^{6} Pa
Compressive strength	SfC	900000.0 psi	6205×10^{6} Pa
Shear strength	SfS	500000.0 psi	3447×10^{6} Pa
Normal damping capacity (11)	psi11f	0.03 %Energy	0.03 %Energy
Normal damping capacity (12)	psi22f	0.4 %Energy	0.4 %Energy
Shear damping capacity (12)	psi12f	0.4 %Energy	0.4 %Energy
Shear damping capacity (23)	psi23f	0.8 %Energy	0.8 %Energy
Melting temperature	TMf	6000.0 °F	3315.6 °C

TABLE 2.—CONVENTIONAL MATRIX (IMHS)
[INTERMEDIATE MODULUS 123M FOR SINGLE FIBER 3–D STRESS ANALYSIS.]

Description	Symbol	Value	Value in SI units
Weight density	Rhom	0.044 lb/in.^{3}	1.218×10^{-6} kg/mm^3
Normal modulus	Em	10000000psi	68.94 GPa.
Poisson's ratio	Num	0.35 non-dim.	0.35 non-dim..
Thermal expansion coefficient	Alfa m	3.6×10^{-5} in./in./°F	6.48×10^{-5} /°C
Heat conductivity	Km	0.008681 BTU/hr/in./°F	1.803×10^{-4}W/mm/°C
Heat capacity	Cm	0.25 BTU/lb/°F	1048 J/kg/°C
Dielectric strength	Kem	0.0 V/in.	0.0 V/mm.
Dielectric constant	Gammam	0.0 in./V	0.0 V/mm.
Capacitance	Cem	0.0 V	0.0 V
Resistivity	Rem	0.0 Ω-in.	0.0 Ω-mm.
Moisture expansion coefficient	Betam	0.0033 in./in./%Moisture	0.0033 /%Moisture
Diffusivity	Dm	2.16×10^{-7} in.^{2}/hr	1.394×10^{-4} mm.^{2}/hr
Saturation	Mm	0.0 %Moisture	0.0 %Moisture
Tensile strength	SmT	15000.0 psi	103.4 MPa
Compressive strength	SmC	35000.0 psi	241.3 MPa
Shear strength	SmS	13000.0 psi	89.63 MPa
Allowable tensile strain	eps mT	0.02 in./in.	0.02 mm./mm.
Allowable compr. strain	eps mC	0.05 in./in.	0.05 mm./mm.
Allowable shear strain	eps mS	0.035 in./in.	0.035 mm./mm.
Allowable torsional strain	eps mTOR	0.035 in./in.	0.035 mm./mm.
Normal damping capacity	psiNm	6.6 %Energy	6.6 %Energy
Shear damping capacity	psiSm	6.9 %Energy	6.9 %Energy
Void heat conductivity	Kv	0.225 BTU/hr/in./°F	4.673×10^{-3} W/mm/°C
Glass transition temperature	Tgdr	420.0 °F	215.6 °C
Melting temperature	TMm	0.0 °F	-17.78 °C

TABLE 3.—NANOFIBER REINFORCED MATRIX
(NFRM—0.01 FIBER REINFORCEMENT)

Description	Symbol	Value	Value in SI units
Weight density	Rhom	0.047 lb/in.^{3}	1.301×10^{-6} kg/mm^3
Normal modulus	Em	6.774×10^7 psi	467.1 GPa.
Poisson's ratio	Num	0.3323 non-dim.	0.3323 non-dim
Thermal expansion coefficient	Alfa m	5.6×10^{-9} in./in./°F	10.08×10^{-9} /°C
Heat conductivity	Km	444.0 BTU/hr/in./°F	9.221 W/mm/°C
Heat capacity	Cm	0.227 BTU/lb/°F	951.1 J/kg/°C
Dielectric strength	Kem	0.0 V/in.	0.0 V/mm.
Dielectric constant	Gammam	0.0 in./V	0.0 V/mm.
Capacitance	Cem	0.0 V	0.0 V
Resistivity	Rem	0.0 Ω-in.	0.0 Ω-mm.
Moisture expansion coefficient	Betam	5.5×10^{-11} in./in./%Moisture	5.5×10^{-11} /%Moisture
Diffusivity	Dm	5.4×10^{-11} in.^{2}/hr	3.484×10^{-8} mm.^{2}/hr
Saturation	Mm	0.0 %Moisture	0.0 %Moisture
Tensile strength	SmT	800000.0 psi	5.516 GPa
Compressive strength	SmC	600000.0 psi	4.137 GPa
Shear strength	SmS	400000.0 psi	2.758 GPa
Allowable tensile strain	eps mT	0.0070 in./in.	0.0070 mm./mm.
Allowable compr. strain	eps mC	0.0060 in./in.	0.0060 mm./mm.
Allowable shear strain	eps mS	0.0040 in./in.	0.0040 mm./mm.
Allowable torsional strain	eps mTOR	0.0040 in./in.	0.0040 mm./mm.
Normal damping capacity	psiNm	0.4 %Energy	0.4 %Energy
Shear damping capacity	psiSm	0.4 %Energy	0.4 %Energy
Void heat conductivity	Kv	0.225 BTU/hr/in./°F	4.673×10^{-3} W/mm/°C
Glass transition temperature	Tgdr	420.0 °F	215.6 °C
Melting temperature	TMm	550.0 °F	287.8 °C

TABLE 4.—CONVENTIONAL FIBER (AS00)

Description	Symbol	Value	Value in SI units
Number of fibers per end	Nf	10000.0	10000.0
Filament equivalent diameter	df	3.0×10^{-4} in.	76.2×10^{-4} mm.
Weight density	Rhof	0.063 lb/in.^{3}	1.744×10^{-6} kg/mm^3.
Normal moduli (11)	Ef11	3.2×10^{7} psi	22.06×10^{10} Pa
Normal moduli (22)	Ef22	2000000.0 psi	13.79 GPa
Poisson's ratio (12)	Nuf12	0.2 non-dim.	0.2 non-dim.
Poisson's ratio (23)	Nuf23	0.25 non-dim.	0.25 non-dim.
Shear moduli (12)	Gf12	2000000.0 psi	13.79 G Pa
Shear moduli (23)	Gf23	1000000.0 psi	6.895 GPa
Thermal expansion coefficient (11)	Alfaf11	5.5×10^{-7} in./in./°F	9.9×10^{-7} /°C
Thermal expansion coefficient (22)	Alfaf22	5.5×10^{-4} in./in./°F	9.9×10^{-4} /°C
Heat conductivity (11)	Kf11	4.03 BTU/hr/in./°F	0.08370 W/mm/°C
Heat conductivity (12)	Kf12	0.403 BTU/hr/in./°F	0.008370 W/mm/°C
Heat capacity	Cf	0.17 BTU/lb/°F	712.3 J/kg/°C
Dielectric strength (11)	Kef11	0.0 V/in.	0.0 V/mm
Dielectric strength (22)	Kef22	0.0 V/in.	0.0 V/mm
Dielectric constant (11)	Gammaf11	0.0 in./V	0.0 mm./V
Dielectric constant (22)	Gammaf22	0.0 in./V	0.0 mm./V
Capacitance	Cef	0.0 V	0.0 V
Resistivity	Ref	0.0 Ω-in.	0.0 Ω-mm
Tensile strength	SfT	400000.0 psi	2.758 GPa
Compressive strength	SfC	350000.0 psi	2.413 GPa
Shear strength	SfS	250000.0 psi	1.724 GPa
Normal damping capacity (11)	psi11f	0.05 %Energy	0.05 %Energy
Normal damping capacity (12)	psi22f	0.25 %Energy	0.25 %Energy
Shear damping capacity (12)	psi12f	0.35 %Energy	0.35 %Energy
Shear damping capacity (23)	psi23f	0.5 %Energy	0.5 %Energy
Melting temperature	TMf	6000.0 °F	3315.6 °C

TABLE 5.—BENDING REGIDITIES OF UNIDIRECTIONAL COMPOSITE FOR BUCKLING ANALYSIS

θ	D_{11}	D_{12}	D_{13}	D_{22}	D_{23}	D_{33}	Comment
0	3.87 + 6	5.41 + 4	0	2.14 + 4	0	2.10 + 4	With NFRM; $k_f = 0.01$
0	1.62 + 6	2.60 + 5	0	9.98 + 4	0	5.19 + 4	Without NFRM
kPa	27.10 + 6	6.08 + 4	0	14.94 + 5	0	14.66 + 5	
kPa	11.31 + 6	18.15 + 5	0	69.60 + 4	0	36.23 + 4	

TABLE 6.—BUCKLING FACTOR RESULTS ON ANISOTROPIC COMPOSITE PLATES WITH CONVENTIONAL MATRIX

Load conditions and buckling factor			
√	0	0	–1793
0	√	0	–529
0	0	√	–1023
√	√	0	–422
√	0	√	–708
0	√	√	–383
√	√	√	–323

TABLE 7.—BUCKLING FACTOR RESULTS OF ANISOTROPIC COMPOSITE PLATES WITH NFRM

Load conditions and buckling factor			
√	0	0	–3673
0	√	0	–1097
0	0	√	–2220
√	√	0	–875
√	0	√	–1523
0	√	√	–808
√	√	√	–680

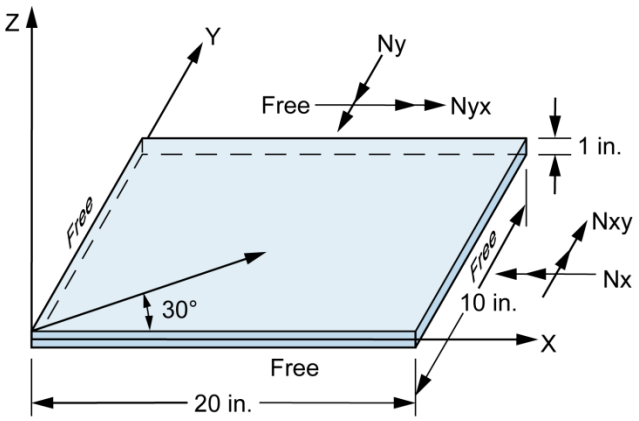

Figure 1.—Anisotropic plate schematic.

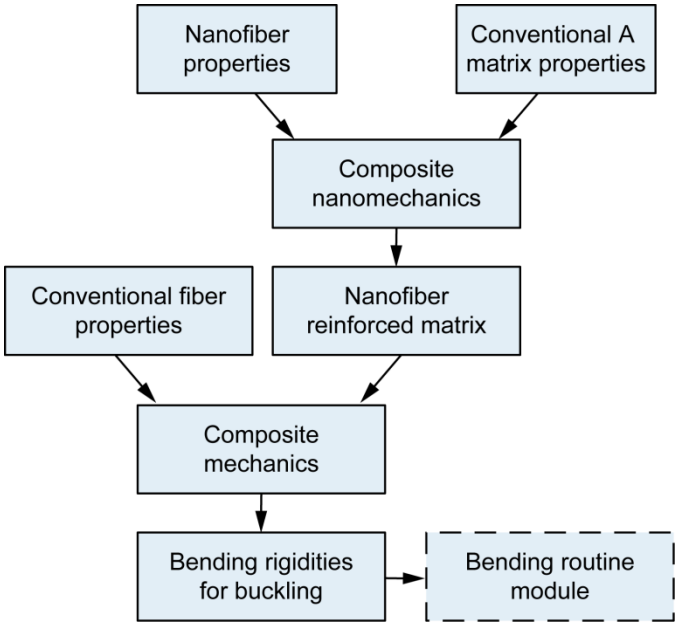

Figure 2.—Simulation of nanofiber reinforced matrix schematic.

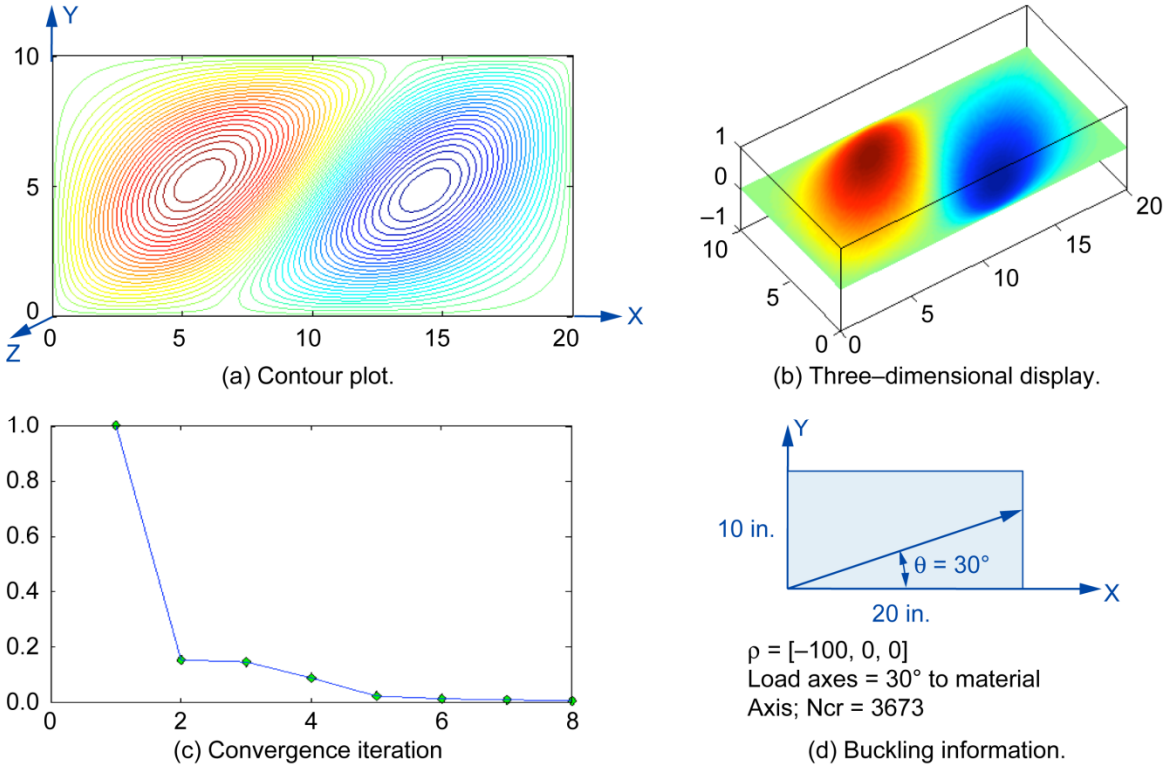

Figure 3.—Buckling mode shapes and convergence of fiber composites anisotropic plates with 0.01 nanofiber reinforced matrix loaded in the structural X–axis.

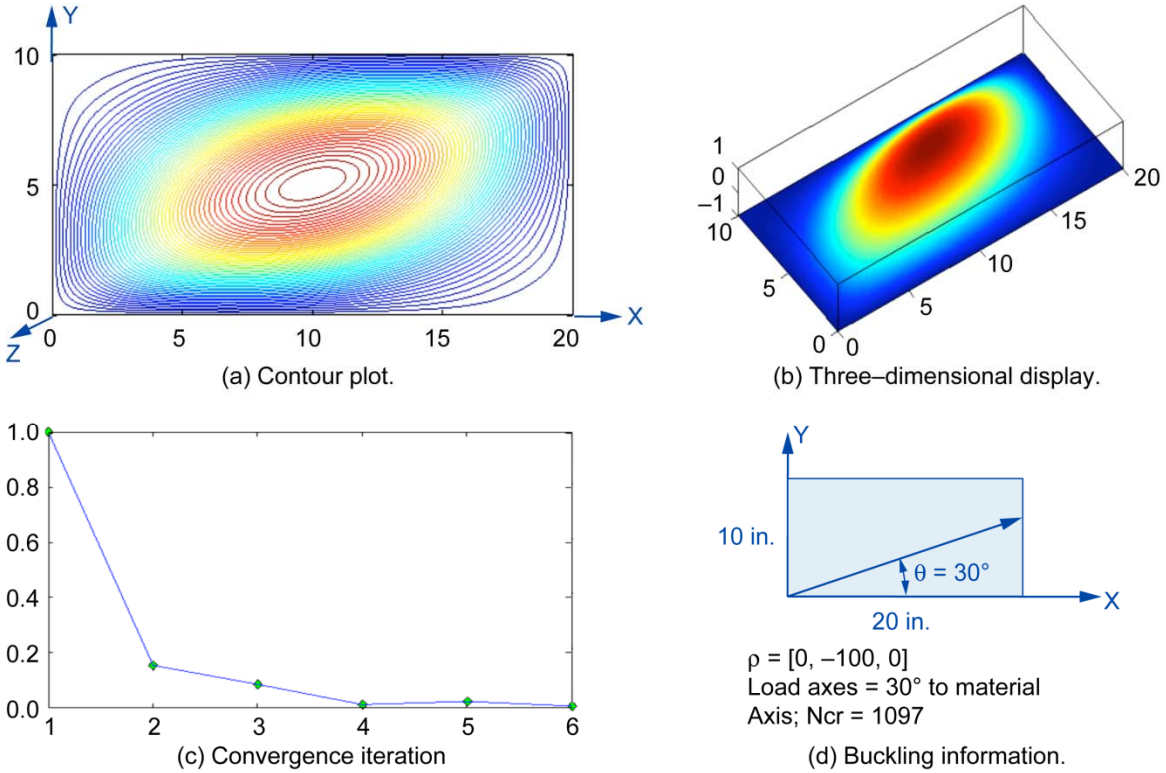

Figure 4.—Buckling mode shapes and convergence of fiber composites anisotropic plates with 0.01 nanofiber reinforced matrix loaded in the structural Y–axis.

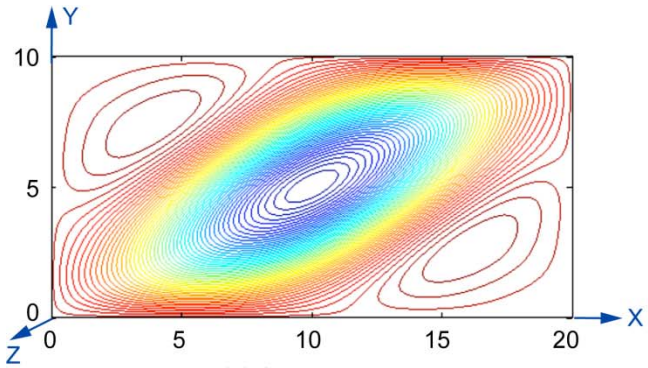

(a) Contour plot.

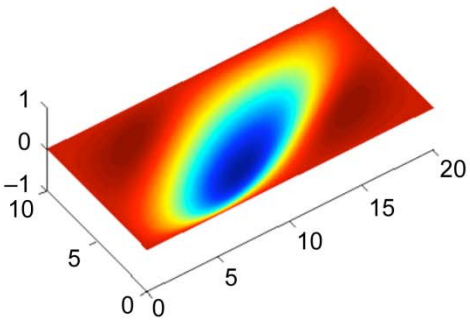

(b) Three–dimensional display.

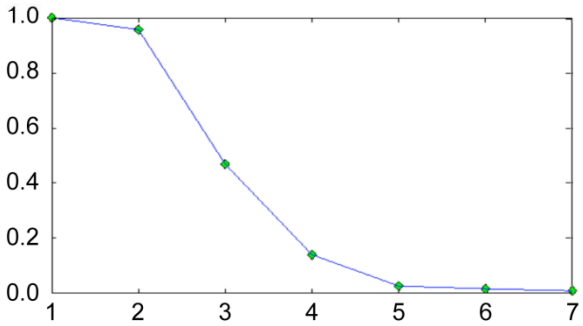

(c) Convergence iteration

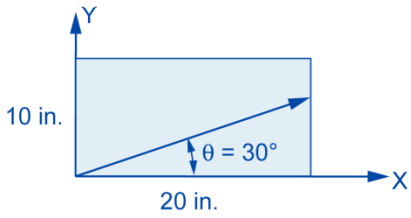

ρ = [–1, –1, –100]
Load axes = 30° to material
Axis; Ncr = 2220

(d) Buckling information.

Figure 5.—Buckling mode shapes and convergence of fiber composites anisotropic plates with 0.01 nanofiber reinforced matrix loaded in the structural XY–axis.

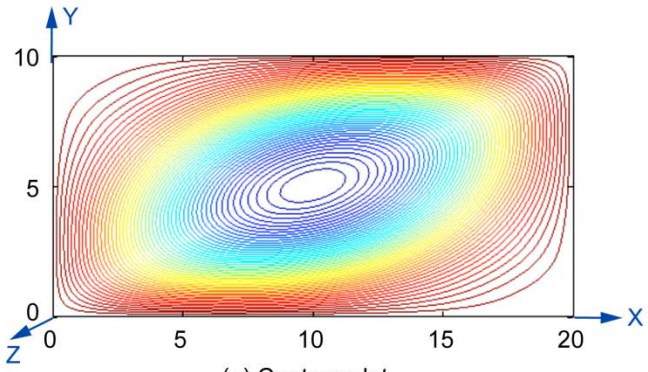

(a) Contour plot.

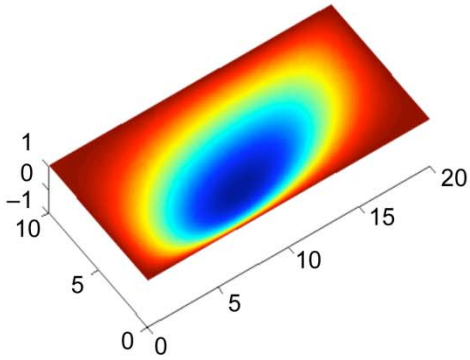

(b) Three–dimensional display.

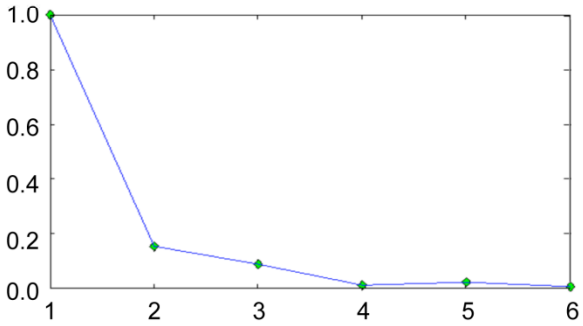

(c) Convergence iteration

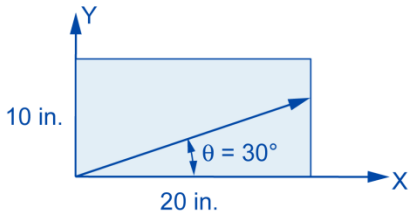

ρ = [–100, –100, 0]
Load axes = 30° to material
Axis; Ncr = 875

(d) Buckling information.

Figure 6.—Buckling mode shapes and convergence of fiber composites anisotropic plates with 0.01 nanofiber reinforced matrix loaded in the structural X and Y–axis.

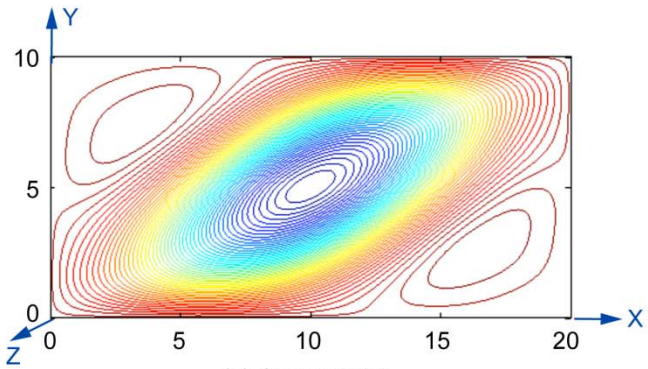

(a) Contour plot.

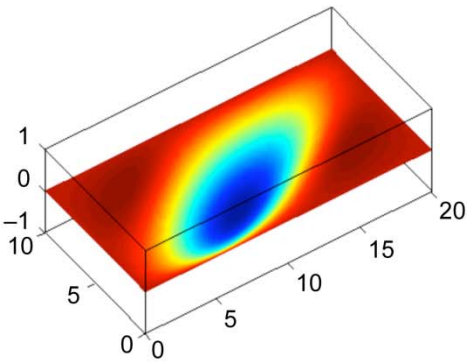

(b) Three–dimensional display.

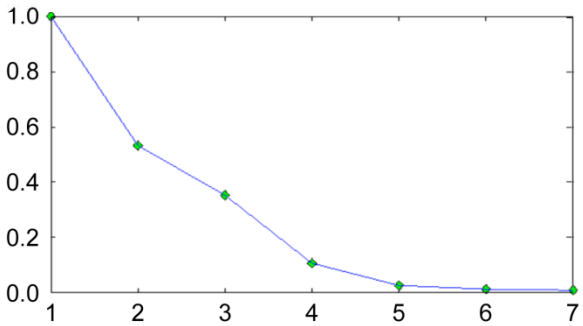

(c) Convergence iteration

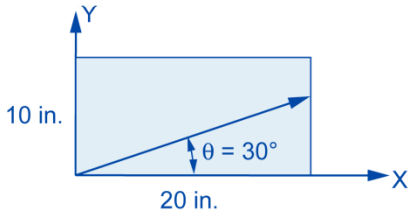

ρ = [–100, 0, –100]
Load axes = 30° to material
Axis; Ncr = 2220

(d) Buckling information.

Figure 7.—Buckling mode shapes and convergence of fiber composites anisotropic plates with 0.01 nanofiber reinforced matrix loaded in the structural X and XY–axis.

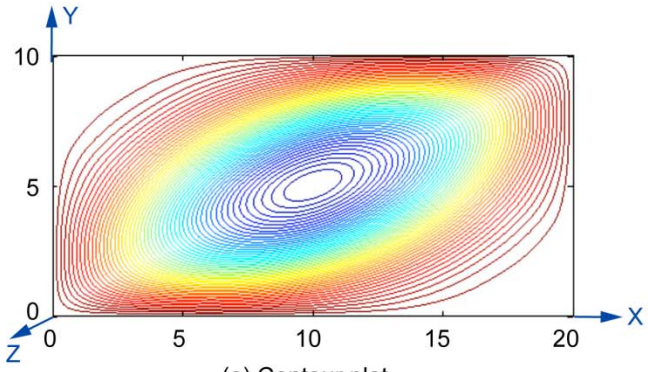

(a) Contour plot.

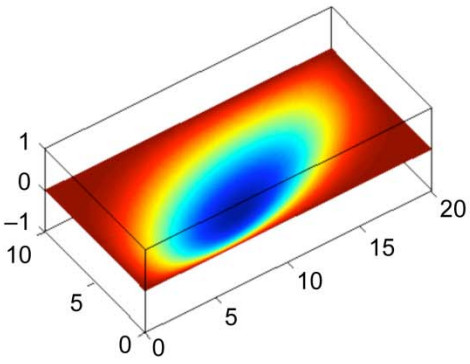

(b) Three–dimensional display.

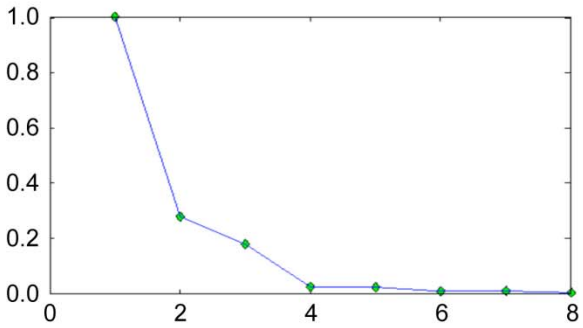

(c) Convergence iteration

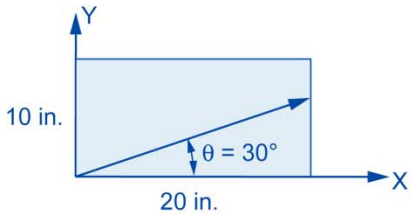

ρ = [0, –100, –100]
Load axes = 30° to material
Axis; Ncr = 808

(d) Buckling information.

Figure 8.—Buckling mode shapes and convergence of fiber composites anisotropic plates with 0.01 nanofiber reinforced matrix loaded in the structural Y and XY–axis.

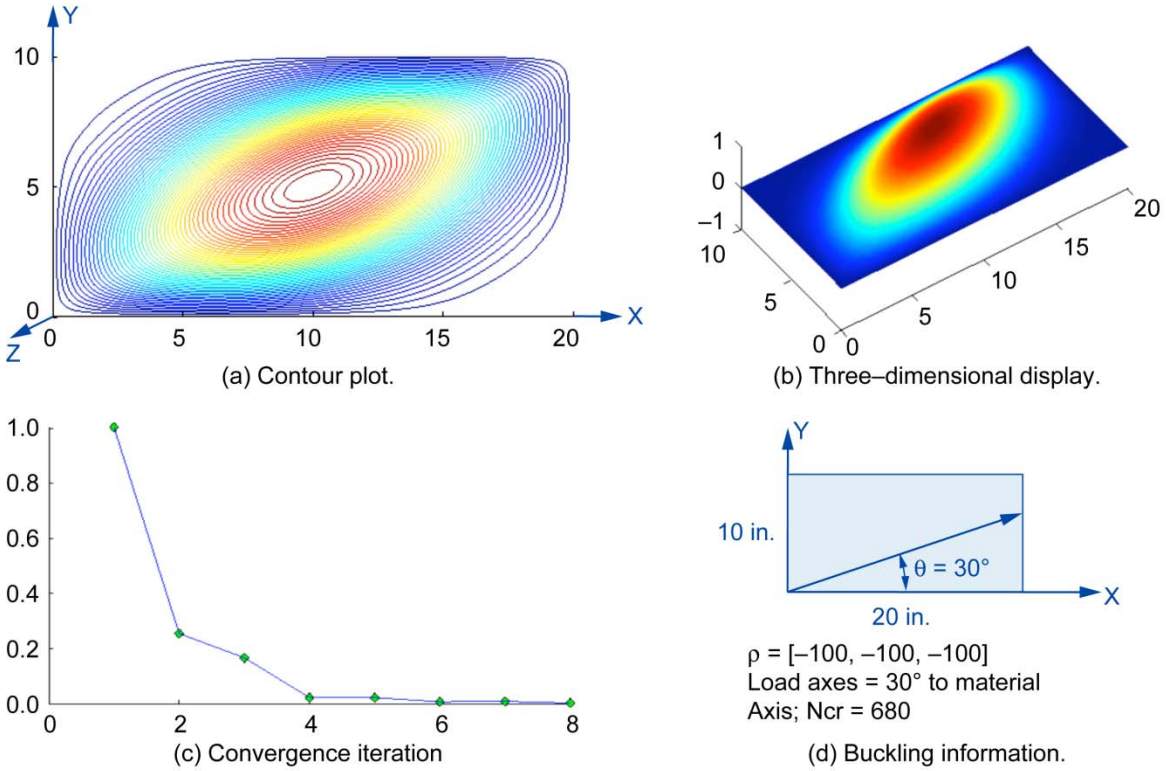

Figure 9.—Buckling mode shapes and convergence of fiber composites anisotropic plates with 0.01 nanofiber reinforced matrix loaded in the structural X and Y and XY–axis.